Journal of ELECTRICAL ENGINEERING, VOL 61. NO 7/s, 2010, 115-118

INVESTIGATION OF MEASURED DISTRIBUTIONS OF LOCAL VECTOR MAGNETIC PROPERTIES IN A THREE-PHASE INDUCTION MOTOR MODEL CORE

Takayuki Kai* — Shigeru Aihara* — Takashi Todaka* — Masato Enokizono*

In this paper, we measured distributions of two-dimensional magnetic properties in a three-phase induction motor model core with a newly developed small-sized vector hysteresis sensor called *V-H* sensor. Additionally, we analyzed distributions of vector magnetic properties in the model core by means of the finite element method considering the E&S modelling. The analyzed results are compared with the measured ones.

Keywords: two-dimensional magnetic properties, vector hysteresis sensor, three-phase induction motor, E&S modelling

1 INTRODUCTION

Three-phase induction motors are widely used in both industrial and domestic fields for their robustness and flexibility. Improvements of their efficiency would lead to significant electrical energy saving. This improvement depends not only on optimizing the motor design but also on the electrical steel quantity. It is well known that the magnetic properties of the electrical steel sheets deteriorate in manufacturing processes of motors, however the local magnetic phenomenon in constructed motor cores has not yet been understood sufficiently.

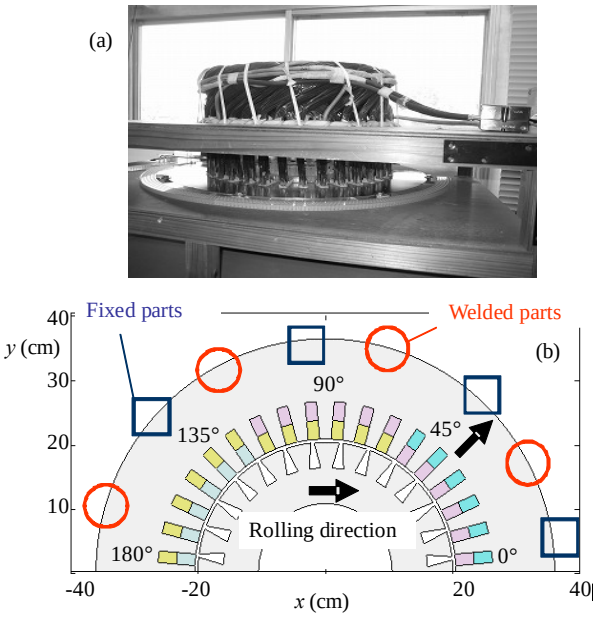

Fig. 1. Three-phase induction motor model core: (a) - Picture of the three-phase induction motor model core, (b) - Diagrammatic illustration of the model core

On the other hand, we have developed a vector hysteresis sensor (*V-H* sensor) by utilizing the double *H*-coil method and the needle-probe method [1], and measured distributions of vector magnetic properties in a three-phase induction motor model core [2]. The vector magnetic property enables us to know the rotational iron loss distributions and magnetic anisotropic properties in the relationship between the flux density vector and the field intensity vector [1].

Recently we have developed a 4mm x 4mm double H-coil by using 0.012mm ultra fine magnet wire and precise alumina ceramic frame. This enabled us more detailed magnetic property measurements in higher resolution at narrow areas such as the tooth part of the model core.

In this paper, we report measured distributions of vector magnetic properties in the three-phase induction motor model core with the new small-sized *V-H* sensor. Particularly we discuss measurement accuracy around tooth part near the exciting windings. Furthermore, the distributions of vector magnetic properties in the model core were analyzed by means of the finite element method considering the E&S modelling [3] and the calculated results were compared with the measured ones. Knowledge obtained in the measurement and analysis can be associated with reduction of building factors.

2 MEASUREMENTS

2.1 Three-phase induction motor model core

Figure 1(a) shows the photograph of the three-phase induction motor model core used in the measurement. Figure 1(b) shows the diagrammatic illustration of the model core. The number of stator slot and rotor slot were equal to 36 and 28, respectively. The material of the model core was 0.5 mm thickness non-oriented silicon steel sheet, and the total number of lamination was equal to 20. The stator winding was a double layer. The number of stator winding in each stator slot was equal to be 5. In order to reduce the influence of the magnetic field from the winding edge, the distance between the winding edge and the core was kept longer about 300mm in distance. In order to measure safety, the rotor core without secondary conductors was fixed on a wooden board, and it could not be rotated. Additionally, the insulating layer

* Department of Electrical and Electronic Engineering, Faculty of Engineering, Oita University, 700 Dannoharu, Oita 870-1192, Japan; v10e2012@oita-u.ac.jp

ISSN 1335-3632

on the upper silicon steel sheet of the laminated core was eliminated to measure magnetic flux density distributions with the needle-probe method. In addition, one search coil was wound around the stator back yoke to measure the average flux density, B_a. The average flux density was controlled to be constant during measurements as an exciting condition (the exciting magnetic flux density).

2.2 VH sensor

Fig.2 shows the construction of the *V-H* sensor. The sensor has the two sets of the needle probe for measuring the magnetic flux density ***B*** in each direction. The distance between the needles was 7 mm. In addition, the sensor has the double *H*-coils for measuring the magnetic field intensity ***H*** in each direction. The H_x-coil was wound over a ceramic flame, and H_y-coil was wound around the H_x-coil. The each number of turns was 350 and we used 0.012mm ultra fine magnet wire to keep sensitivity. The effective area turns of the H_x-coil and the H_y-coil were equal to be $525\text{x}10^{-6}$ mm^2-turn and $791\text{x}10^{-6}$ mm^2-turn, respectively. The components of the magnetic flux density ***B*** and the magnetic field intensity ***H*** are calculated by

$$H_i = \frac{1}{\mu_0 S_{Hi} N_{Hi}} \int_0^T e_{H_i} dt \tag{1}$$

$$B_i = \frac{2}{S_{Bi}} \int_0^T e_{B_i} dt \tag{2}$$

where, e_{Bi} and e_{Hi} are the induced voltages of the needle probe and the *H*-coil, respectively. S_{Bi} and $S_{Hi}N_{Hi}$ are the effective area turns. Here, T is the period of exciting waveform.

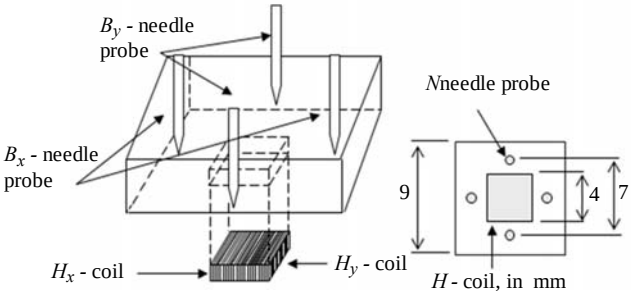

Fig. 2. New vector hysteresis sensor (*V-H* sensor)

2.3 Measurement system

Figure 3 shows the block diagram of the measurement system to measure the vector magnetic properties in the three-phase induction motor model core. The three-phase excitation voltage outputted from the D/A converter was amplified with the power amplifier and supplied to the excitation coils. The three-phase excitation voltage was also controlled by feedback to be a certain average magnetic flux density, B_a, which measured with the search coil wound around the stator core-back. In this measurement, the maximum value of B_a and the exciting frequency were set to be 0.2 T and 50 Hz, respectively. Furthermore, the number of the sampling points, the sampling frequency, and the number of the measured points were 20000, 1MHz, and 3800, respectively. These enabled us more detailed vector magnetic property measurements in higher resolution.

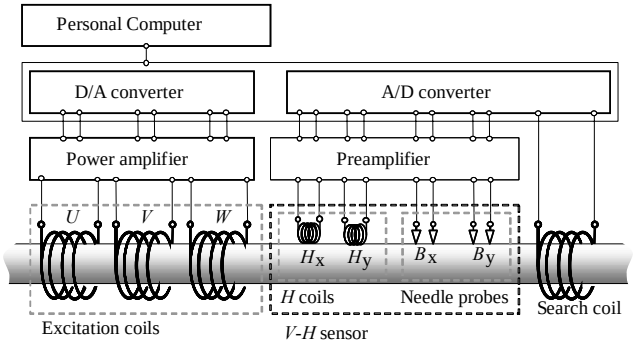

Fig. 3. Measurement system

3 MEASURED RESULTS

3.1 Distribution of the maximum magnetic flux density, the maximum field intensity, and iron loss

Figure 4 shows the distributions of the maximum magnetic flux density and the maximum field intensity. As shown in Fig. 4(a) and (b), large ***B*** and comparatively smaller ***H*** were observed at place where the principal magnetic flux density vector was parallel to the rolling direction of the core material. The rolling direction was indicated with arrows in Fig. 1(b). Contrary, smaller ***B*** and comparatively larger ***H*** were observed at a place where the principal magnetic flux density vector was perpendicular to the rolling direction. This is caused by the magnetic anisotropy of the core material due to rolling. Although the core material is one of the non-oriented silicon steel sheets, the magnetic permeability in the rolling direction is about 1.5 times larger than that in the transverse direction. Furthermore, we can confirm small ***B*** at the welded parts and large ***B*** at the stator core-back near the welded parts. The magnetic flux of the stator core-back avoided the welded parts and went through more inside path.

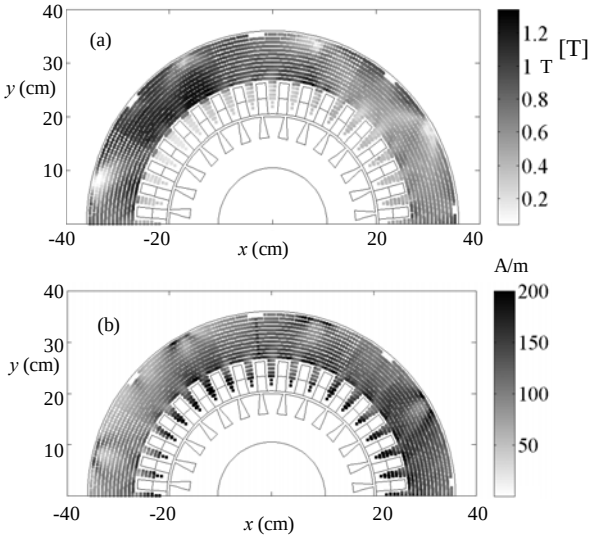

Fig. 4. Distributions of: (a) - the maximum magnetic flux density, (b) - maximum magnetic field intensity

Figure 5 shows the distribution of iron loss, the iron loss was calculated with the following equation.

$$P_t = \frac{1}{\rho T}\int_0^T \left(H_x \frac{dB_x}{dt} + H_y \frac{dB_y}{dt} \right) dt \qquad (3)$$

where, T is the period of the exciting waveform, ρ is the material density. As shown in Fig. 5, at the region-1 indicated by the dotted circle, the large iron loss was generated by the large ***B*** and the large ***H***. Additionally, the iron loss distribution was similar to that of the maximum magnetic flux density distribution. However, at the region-2, the large iron loss was generated by the small ***B*** and large ***H***. It is caused by the anisotropy of magnetic materials. It is necessary to evaluate the iron loss distribution considering the local vector magnetic properties by using the *V-H* sensor.

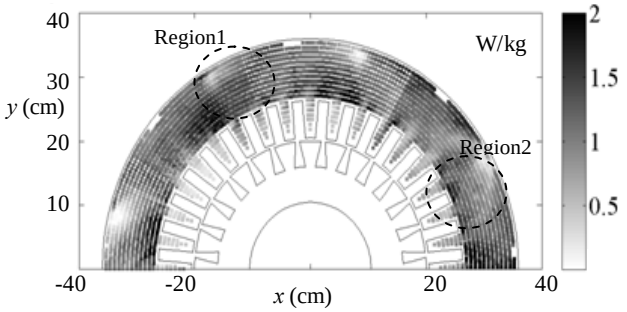

Fig. 5. Distribution of the iron loss

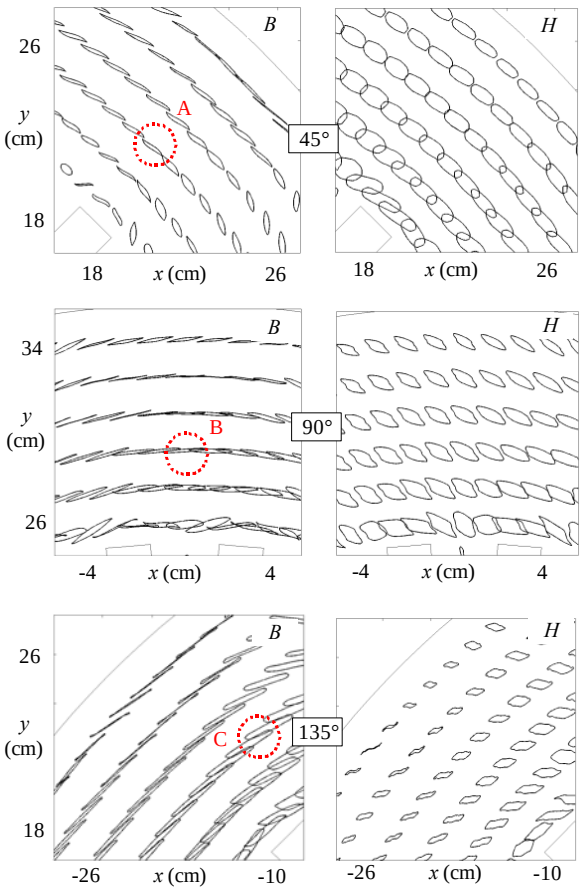

Fig. 6. Distributions of the rotating magnetic flux density and field intensity vector trajectories in the stator back yoke

3.2 Distribution of rotating magnetic flux density and the field intensity at the stator core-back

Figure 6 shows distribution of the rotating magnetic flux density and magnetic field intensity vector trajectories at the each stator back yoke. Figure 7 shows two-dimensional vector magnetic properties measured at the points A, B and C defined in Fig. 6. As shown in Fig. 6(a) and (b), at 45 degrees, the long principal axes of the rotating magnetic flux density vector trajectories were short, and the long principal axes of the rotating magnetic field intensity vector trajectories were longer in comparison with ones at the other parts. Inversely, as shown in Fig. 6(e) and (f), at 135 degrees, the long principal axes of the rotating magnetic flux density trajectories were long, and the long principal axes of the rotating magnetic field intensity trajectories were short.

On the other hand, as shown Fig. 6(d) and 6(f), at 90 and 135 degrees, the rotating magnetic field intensity trajectories were distorted due to the non-linear relationship between the magnetic flux density and the magnetic field intensity in high inductions.

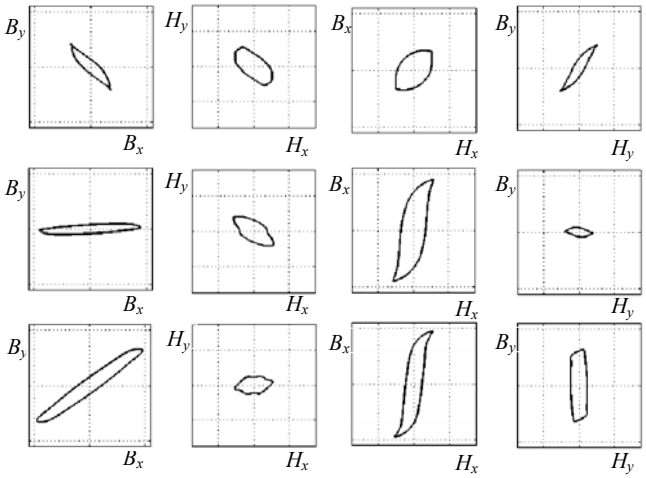

Fig. 7. Two-dimensional vector magnetic properties at points A, B, C row by row; Scale $B \in$ (-1,1) in T, $H \in$ (-200,200) A/m

3.3 Measurement of the stator tooth

Figure 8 shows the distributions of the rotating magnetic flux density and magnetic field intensity vector trajectories at the stator tooth at 40 degrees. It was observed that very large rotating magnetic field at the top of the stator tooth. Additionally, from the root toward the top of the tooth, the rotating magnetic field trajectory shape was gradually changed from alternating field to rotating field. At the other top of the teeth, large rotating magnetic field was also observed.

Figure 9 shows the measured magnetic flux and field intensity waveforms, which are transformed into the radial and circumferential component at each measurement position. As shown in this figure, toward the top of the tooth, the amplitude of B_r was increased and B_θ was decreased. Similarly, the amplitude of H_r was increased and H_θ was decreased. at the same time the phase of H_θ was

changed about 180 degrees. It seems that the field intensity signals are sensitively influenced by the position of the fixed rotor slots and the leakage flux from the exciting coils.

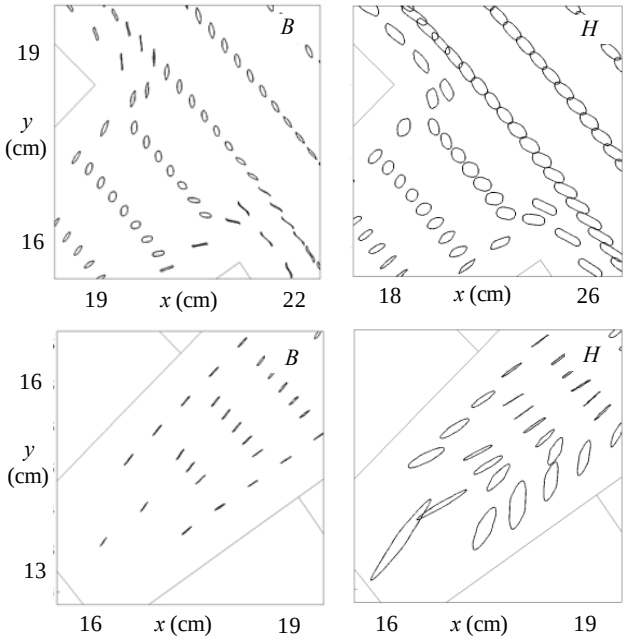

Fig. 8. Distributions of the rotating magnetic flux density and magnetic field intensity vector trajectories in the tooth at 40 deg

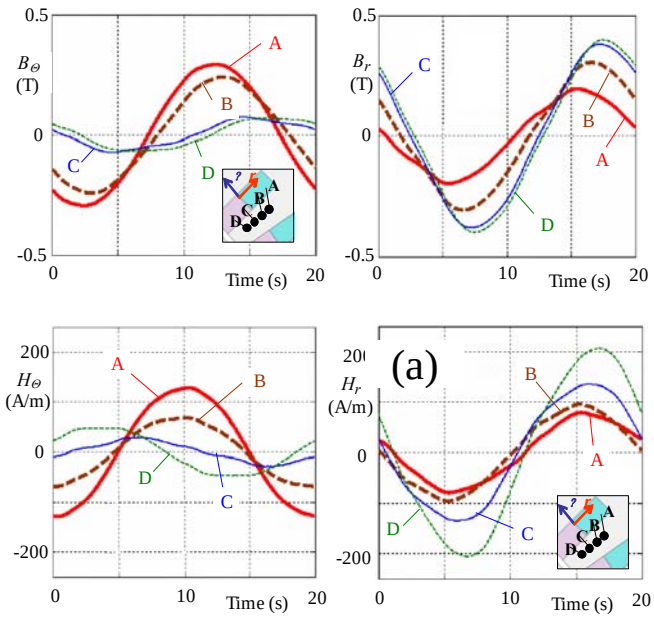

Fig. 9. Components of the ***B*** and ***H*** in points A,B,C,D

3.4 Finite Element Analysis

We carried out magnetic characteristic analysis of the model core by means of the two-dimensional finite element method considering the E&S modeling and the calculated results were compared with the measured ones. Figure10 shows the calculated results. As shown in this figure, the large rotating magnetic flux density and magnetic field intensity vector trajectories were generated at the roots of teeth. We could also confirm in the two-dimensional approximation that the magnetic flux density and magnetic field intensity were almost alternating in the stator tooth. The magnetic field intensity at the top of the teeth was larger than one at the middle part.

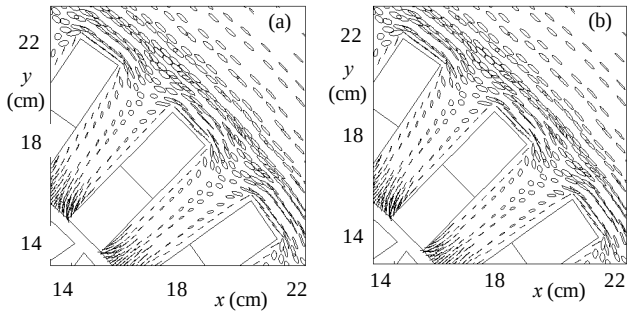

Fig. 10. Distributions of the trajectories analyzed by FEM considering (E&S modeling): (a) - trajectory of *B*, (b) - trajectory of *H*

4 CONCLUSIONS

The local two-dimensional magnetic properties in the three-phase induction motor model core were measured by using the small-sized vector hysteresis sensor (*V-H* sensor). The small-sized *V-H* sensor enabled us more detailed magnetic property measurements in higher resolution. As analyzed result, we confirmed alternating magnetic flux density and alternating magnetic field intensity in the stator teeth. However, the rotating magnetic field intensity was measured at the top of teeth. As measurement results, although the core material was the non-oriented silicon steel sheet, the clear influence of the magnetic anisotropy due to rolling was observed. The clear influence of the welded parts was also observed. Because the large iron loss is generated by large ***H*** even though small ***B***, the developed *V-H* sensor which can measure local ***B*** and ***H*** at any points is very useful to make clear practical iron loss distributions of rotating machines.

REFERENCES

[1] K. Senda, M. Ishida, K. Sato, M. Komatubara, T. Yamaguchi: Localized Magnetic Properties in Grain-oriented Silicon Steel Measured by Stylus Probe Method. T.IEE of Japan, Vol.117-A, No.9,1997.

[2] M. Enokizono, M. Morioka, K. Kawamura, J. Sievert: Distribution of Two-dimensional Magnetic Properties in Three-Phase Induction Motor Model Core. IEEE Transactions on Magnetics, Vol.32, No.5, 1996.

[3] S. Urata, M. Enokizono, T. Todaka and H. Simoji : Magnetic Characteristic Analysis of the Motor Considering 2-D Vector Magnetic Property, IEEE Transactions on Magnetics,2006

Received 30 September 2010